# Prediction of the mass burning rate of stretched flames including preferential diffusion effects

# Prediction of the mass burning rate of stretched flames including preferential diffusion effects

J.A.M. de Swart*, G.R.A. Groot, J.A. van Oijen, J.H.M. ten Thije Boonkkamp
and L.P.H. de Goey
Department of Mechanical Engineering
Department of Mathematics and Computer Science,
Eindhoven University of Technology
P.O. Box 513, 5600 MB Eindhoven, The Netherlands

**Abstract**

This study focusses on the effect of flame stretch on the mass burning rate, for premixed laminar flames with non-unit Lewis numbers. For the first time detailed chemistry and multi-species transport models are used to check whether these models are applicable to real flames. The adjusted model will be evaluated at the inner reaction layer position. The preferential diffusion effect of methane/air mixtures is more difficult to predict accurately compared to ethane/air and propane/air mixtures, because cancelation of different contributions takes place. This model is a basis for the first quantitative model to predict mass burning rates of premixed, laminar, stretched flames with non-unit Lewis numbers.

## Introduction

It is well-known that flame stretch is a very important quantity in combustion science. A number of studies have been performed, like [1, 7]. Recently, De Goey and Ten Thije Boonkkamp [8] derived a premixed flamelet model from the full set of 3D time dependent conservation equations. From these flamelet equations, a general expression for the influence of flame stretch and preferential diffusion has been derived from first principles extending the integral analysis, introduced by Chung and Law [7]. It is expected that this model can be used as a basis for a quantitative model describing the influence of flame stretch and preferential diffusion on premixed flame dynamics. In previous studies it has been shown already that this model accurately describes the influence of flame stretch on premixed laminar flames [9], partially premixed triple flames [10] and even in case of highly stretched turbulent flames [11] for the case of unit Lewis-numbers. The application of the theory to detailed chemistry has not been studied so far. The focus of this paper is on this aspect for the case of weakly stretched planar flames. In the future, the application to strong stretch will be analyzed. This might open the way to describe the mass burning rate of turbulent flames without solving the complete flame structure.

First, in the next section, the basic model of De Goey and Ten Thije Boonkkamp will be adjusted to describe the influence of flame stretch on the mass burning rate at the inner reaction layer rather than at the burnt side of the flame. It is known that preferential diffusion in combination with flame stretch introduces a change in the element composition and enthalpy at the inner reaction layer. Detailed models for these phenomena are presented in the subsequent section. The accuracy of the predicted mass burning rate as a function of the change in enthalpy and the element mass fractions and flame stretch will be analyzed and compared with direct numerical results. Deviations between theory and numerical simulations will also be identified. The paper ends with conclusions from the analysis.

## Mass burning rate of stretched flames

Based on the full set of 3D instationary conservation equations for deflagration processes, De Goey and Ten Thije Boonkkamp [8] derived a set of flamelet equations for premixed flames. The flame is defined in terms of iso-surfaces of a progress variable $\mathcal{Y}$ and a local orthogonal coordinate transformation is used to define a coordinate $s$ perpendicular to these surfaces. The resulting equations read:

$$\frac{\partial}{\partial s}(\sigma m) = -\sigma\rho K \,, \tag{1}$$

$$\frac{\partial}{\partial s}(\sigma m Y_i) - \frac{1}{Le_i}\frac{\partial}{\partial s}\left(\sigma\frac{\lambda}{c_p}\frac{\partial Y_i}{\partial s}\right) - \sigma\omega_i = -\sigma\rho K Y_i \qquad (i = 1, \ldots, N_s - 1) \,, \tag{2}$$

$$\frac{\partial}{\partial s}(\sigma m h) - \frac{\partial}{\partial s}\left(\sigma\frac{\lambda}{c_p}\frac{\partial h}{\partial s}\right) - \left(\frac{1}{Le_i} - 1\right)\frac{\partial}{\partial s}\left(\sum_{i=1}^{N_s}\sigma h_i\frac{\lambda}{c_p}\frac{\partial Y_i}{\partial s}\right) = -\sigma\rho K h \,. \tag{3}$$

The element mass fraction $Z_j$ of element $j$ is defined by:

*Corresponding author: j.a.m.d.swart@tue.nl
Associated Web site: http://www.combustion.tue.nl
Proceedings of the European Combustion Meeting 2005

$$Z_j = \sum_{i=1}^{N_s} W_{ji} Y_i \,, \tag{4}$$

with $W_{ji}$ the mass of element $j$ per mass of species $i$. By taking a suitable linear combination of Eq. 2, we obtain:

$$\frac{\partial}{\partial s}(\sigma m Z_j) - \frac{\partial}{\partial s}\left(\sigma \frac{\lambda}{c_p}\frac{\partial Z_j}{\partial s}\right) - \left(\frac{1}{Le_i} - 1\right)\frac{\partial}{\partial s}\left(\sum_{i=1}^{N_s} \sigma W_{ji}\frac{\lambda}{c_p}\frac{\partial Y_i}{\partial s}\right) = -\rho K Z_j \,. \tag{5}$$

The flame stretch rate is defined as the relative rate of change of mass in a small control volume inside the flame structure [12]:

$$K = \frac{1}{M}\frac{\mathrm{d}M}{\mathrm{d}t} \,. \tag{6}$$

Physically this represents the mass flow along the isosurfaces.

Transport terms along the flame surfaces are gathered in the terms proportional to $\rho K$. Here, $\rho$ and K are the mass density and the mass-based flame stretch rate, respectively. Furthermore, $\sigma$ is an area function, in this study equal to one ($\sigma = 1$) because we consider planar flames here. Terms due to non-steady effects in the flame adapted coordinate system and arising because local isosurfaces of the variables $Y_i$, $h$ and $Z_j$ do not necessarily coincide, are neglected. This is valid when the flame structure is thin compared to external distortions. In the above equations $m = \rho s_L$ is the mass burning rate, $s_L$ the burning velocity, $Y_i$ is the mass fraction of species $i$, $Le_i$ is the constant Lewis-number of species $i$, $\lambda$ is the thermal conductivity, $c_p$ is the specific heat at constant pressure, $\omega_i$ is the chemical source term of species $i$ and $h$ is the specific enthalpy. This specific enthalpy can be split in two parts:

$$h = h_T + \sum_{i=1}^{N_s} h_i^{form} Y_i \,, \tag{7}$$

with $h_T$ the thermal enthalpy and the second term on the right hand side the enthalpy of formation. The thermal part of the specific enthalpy in Eq. 7 can be defined as:

$$h_T = \int_{T_{ref}}^{T} \sum_{i=1}^{N_s} c_{p,i}(\xi) Y_i \mathrm{d}\xi = \int_{T_{ref}}^{T} c_p(\xi)\mathrm{d}\xi \,. \tag{8}$$

From the flamelet equations an expression for the mass burning rate at the burnt side of an unstretched premixed flame has been derived [8]. For planar flames this reduces to:

$$m_b^0 \approx \mathcal{F}\left(\mathcal{Y}_u, h_b^0, \mathbf{Z}_b^0\right) , \tag{9}$$

with:

$$\mathcal{F}\left(\mathcal{Y}_u, h_b^0, \mathbf{Z}_b^0\right) = \frac{1}{|\mathcal{Y}_b^0 - \mathcal{Y}_u|}\sqrt{2\int_{\mathcal{Y}_u}^{\mathcal{Y}_b^0} \frac{1}{Le_{\mathcal{Y}}}\frac{\lambda}{c_p}\omega_{\mathcal{Y}}\mathrm{d}\mathcal{Y}} \tag{10}$$

where subscripts $u$ and $b$ indicate the unburnt and the burnt situation, respectively and where $\mathbf{Z}$ is a shorthand notation for $Z_1, \ldots, Z_{N_e}$. Superscript 0 refers to the unstretched situation. The mass burning rate of a stretched flame is given by:

$$m_b\left(\mathcal{Y}_u, h_b, \mathbf{Z}_b\right) = \mathcal{F}\left(\mathcal{Y}_u, h_b, \mathbf{Z}_b\right) - \int_{s_u}^{s_b} \rho K \tilde{\mathcal{Y}} \mathrm{d}s \,, \tag{11}$$

in which the scaled progress variable $\tilde{\mathcal{Y}}$ is defined as:

$$\tilde{\mathcal{Y}} = \frac{\mathcal{Y} - \mathcal{Y}_u}{\mathcal{Y}_b - \mathcal{Y}_u} \,, \tag{12}$$

with $0 \leq \tilde{\mathcal{Y}} \leq 1$. Here $\tilde{\mathcal{Y}} = 0$ indicates the unburnt situation and $\tilde{\mathcal{Y}} = 1$ indicates the burnt situation. Note the difference between $m_b\left(\mathcal{Y}_u, h_b, \mathbf{Z}_b\right)$ and $m_b\left(\mathcal{Y}_u, h_b^0, \mathbf{Z}_b^0\right)$. Also the expression for the mass burning rate $m_b$ for a stretched flame has an extra term (last term in Eq. 11) to compensate for flame stretch, even if $Le_i = 1$. The preferential diffusion contributions are hidden in the other term with $m_b^0\left(\mathcal{Y}_u, h_b, \mathbf{Z}_b\right)$. The chemical species and enthalpy will be redistributed in the flame zone because the diffusion velocity differs for each chemical component. The diffusivity of each component is characterized by its Lewis-number, which means that preferential diffusion is related to non-unit Lewis-numbers. For weak stretch it is possible to expand the term $m_b^0(\mathcal{Y}_u, h_b, \mathbf{Z}_b)$ around $m_b^0(\mathcal{Y}_u, h_b^0, \mathbf{Z}_b^0)$. De Goey et al. then found:

$$\frac{m_b}{m_b^0} \approx 1 - \frac{Ka_{\mathcal{Y}}}{Le_{\mathcal{Y}}} + \Delta h_b \frac{\partial}{\partial h_b^0}\left(\ln m_b^0\right) + \sum_{j=1}^{N_e-1} \Delta Z_{j,b}\frac{\partial}{\partial Z_{j,b}^0}\left(\ln m_b^0\right) + h.o.t. \tag{13}$$

in which the Karlovitz integral, $Ka_{\mathcal{Y}}$, is defined as:

$$Ka_{\mathcal{Y}} = \frac{Le_{\mathcal{Y}}}{m_b^0}\int_{s_u}^{s_b} \rho K \tilde{\mathcal{Y}} \mathrm{d}s \,. \tag{14}$$

This study will focus on weak stretch, which means that the stretched flame structure and the unstretched flame structure are assumed equal. To arrive at Eq. 13 it has been assumed that the chemical source term is only important in a thin reaction layer within the total structure. Furthermore, the source term depends in a complicated way on all species mass fractions. However, it is known that the reacting paths in composition space are attracted

to a one-dimensional manifold close to the equilibrium point [13].

The inner layer is physically more relevant than the burnt side (equilibrium) of the flame which is located a number of flame thicknesses away from the inner reaction layer. This inner layer is the region where most chemical reactions take place. So the mass burning rate at the inner layer gives a better representation of the propagation speed of the flame than any other position. As a consequence, we expect that the enthalpy and element composition close to the inner layer determines the burning velocity rather than the burnt side composition. It will be shown that predictions of the mass burning rate are most accurate using information from the inner layer position. The resulting equation for the mass burning rate at the inner layer for weakly stretched flames reads:

$$\frac{m_{il}}{m_{il}^0} = 1 - \frac{Ka_{\mathcal{Y},il}}{Le_{\mathcal{Y}}} + \Delta h_{il} \frac{\partial}{\partial h_{il}^0} \left(\ln\ m_{il}^0\right) + \sum_{j=1}^{N_e-1} \Delta Z_{j,il} \frac{\partial}{\partial Z_{j,il}^0} \left(\ln\ m_{il}^0\right) + h.o.t. \quad (15)$$

in which the adjusted Karlovitz integral, $Ka_{\mathcal{Y},il}$, is now defined as:

$$Ka_{\mathcal{Y},il} = \frac{Le_{\mathcal{Y}}}{m_{il}^0} \int_{s_u}^{s_b} \rho K \left\{\tilde{\mathcal{Y}} - H\left(s - s_{il}\right)\right\} \mathrm{d}s\,, \quad (16)$$

where $H(s-s_{il})$ is the Heaviside function. Equation 15 is the core of the adjusted model. Under the assumptions of one-step chemistry, a single Lewis number, exponential temperature and species-profiles in the flame and a thin reaction layer, De Goey et al. [8] found expressions for the Markstein number that were also found by Joulin and Clavin [14] and Clavin [15].

**The influence of stretch on the enthalpy and element mass fractions**

The mass burning rate of a stretchless adiabatic planar flame, $m_{il}^0$ changes if the enthalpy or element composition is adapted, although being conserved in the flame contrary to a stretched flame. For convenience the sensitivity coefficients will be written as follows:

$$c_h = \frac{\partial}{\partial h_{il}^0} \left(\ln\ m_{il}^0\right)\,, \quad (17)$$

for the enthalpy and

$$c_j = \frac{\partial}{\partial Z_{j,il}^0} \left(\ln\ m_{il}^0\right)\,, \quad (18)$$

for element index $j = \mathrm{C}, \mathrm{O}, \mathrm{H}$. Note that there are only $N_e - 1$ independent element fraction changes. The change of the last element mass fraction — in our case that of nitrogen $\Delta Z_{\mathrm{N}}$ — is given by

$$\Delta Z_{N_e} = -\sum_{j=1}^{N_e-1} \Delta Z_j. \quad (19)$$

A numerical approach is used to determine the values of the coefficients $c_h$ and $c_j$ as follows. Input parameters have been changed in stretchless (numerical) flames, which results in different values for $\Delta h$ and $\Delta Z_j$. A least squares fit is used to determine the coefficients $c_h$ and $c_j$. The results are presented in table 1.

Table 1: Sensitivity coefficients at inner layer

| variable | methane | | ethane | propane |
|---|---|---|---|---|
| | $\phi = 0.8$ | $\phi = 0.9$ | $\phi = 0.8$ | $\phi = 0.8$ |
| $c_h$ | 1.5 | 1.2 | 1.2 | 1.5 |
| $c_{\mathrm{C}}$ | 36.8 | 23.3 | 34.6 | 33.9 |
| $c_{\mathrm{O}}$ | 3.1 | 6.9 | $-2.1$ | 3.4 |
| $c_{\mathrm{H}}$ | 104.0 | 154.3 | 142.2 | 147.1 |

It can be seen that the coefficient values are almost independent of the fuel and stoichiometric ratio. This might imply that the fuel breaks up fast and then follows a universal path, which is approximately the same for different hydrocarbon fuels. This corresponds to the low-dimensional manifold theories [13]. This is an interesting result and requires further study.

Expressions presented by [8] for $\Delta h$ and $\Delta Z_j$ were improved in [9], resulting in:

$$h^0(s) - h_u(s) = \frac{\mathcal{D}_h^0}{m^0}\,, \quad (20)$$

and for the stretched flame:

$$h(s) - h_u(s) = -\frac{1}{m} \int_{s_u}^{s} \rho K \left(h - h_u\right) \mathrm{d}s + \frac{\mathcal{D}_h}{m}\,, \quad (21)$$

with $\mathcal{D}_h^0$ the diffusive fluxes in the unstretched and $\mathcal{D}_h$ diffusive fluxes in the stretched situation at position $s$. The diffusive fluxes are defined as:

$$\mathcal{D}_h = \frac{\lambda}{c_p} \frac{\partial h}{\partial s} + \sum_{i=1}^{N} h_i \left(\frac{1}{Le_i} - 1\right) \frac{\lambda}{c_p} \frac{\partial Y_i}{\partial s}\,. \quad (22)$$

Subtracting Eq. 20 from Eq. 21 leads to:

$$\Delta h(s) = -\frac{1}{m} \int_{s_u}^{s} \rho K \left(h - h_u\right) \mathrm{d}s + \frac{\mathcal{D}_h}{m} - \frac{\mathcal{D}_h^0}{m^0}\,. \quad (23)$$

In Eq. 23 no approximations have been introduced, so this equation is exact. It is subsequently assumed that the difference in diffusive fluxes of the unstretched and the stretched flame is negligible. This means that Eq. 23 reduces to:

$$\Delta h(s) \approx -\frac{K}{m^0} \int_{s_u}^{s} \rho^0 \left(h^0 - h_u\right) \mathrm{d}s\,, \quad (24)$$

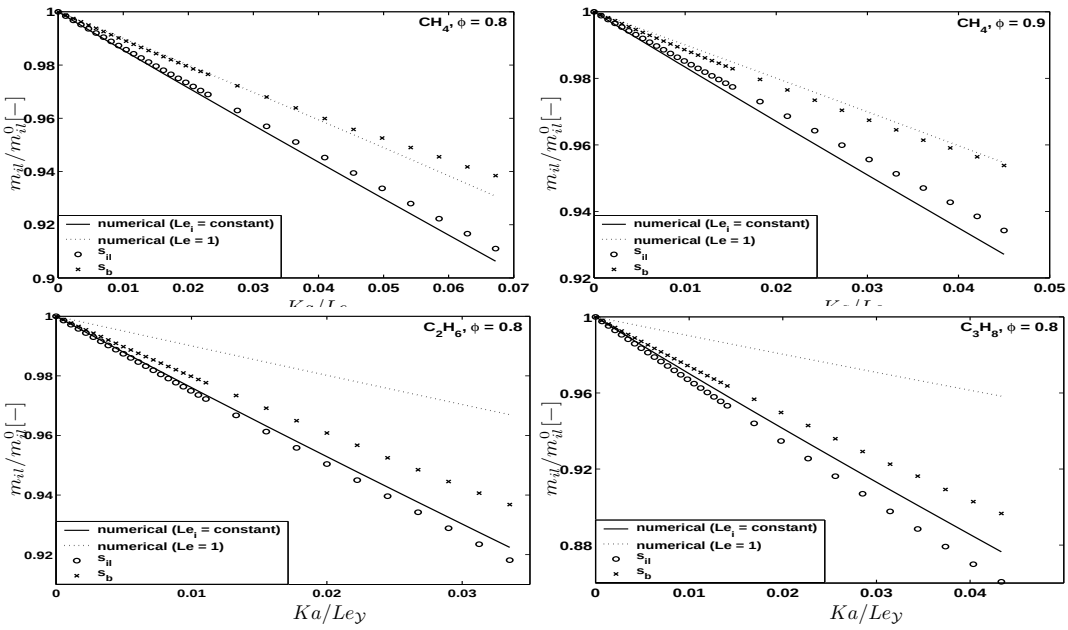


Figure 1: Prediction of $m_{il}/m_{il}^0$ with $\Delta h$ and $\Delta Z_j$ evaluated at $s_{il}$ and $s_b$

where the weak-stretch assumption has been inserted as well. The same approach can be followed for the element mass fraction changes, which yields:

$$\Delta Z_j(s) \approx -\frac{K}{m^0} \int_{s_u}^{s} \rho^0 \left(Z_j^0 - Z_{j,u}\right) \mathrm{d}s \,. \tag{25}$$

Figure 1 shows that predictions of $m_{il}$ with $\Delta h$ and $\Delta Z_j$ evaluated at the inner layer are more accurate than predictions at the burnt side. This confirms the idea that $\Delta h_{il}$ and $\Delta Z_{j,il}$ are more representative than $\Delta h_b$ and $\Delta Z_{j,b}$. Therefore, it is decided to evaluate $\Delta h$ and $\Delta Z_j$ at the inner layer position.

**Accuracy of the model for** $m_{il}$

Finally, the model for the stretched mass burning rate is compared to the numerical solution in figure 2. The scaled mass burning rate is displayed as a function of the Karlovitz integral (scaled with the constant Lewis number), which is defined in Eq. 16. For all types of flames the flame stretch rate varies from $K = 0$ to $K = 300\ 1/\mathrm{s}$. The Karlovitz integral is always smaller than 0.1. In the low $K$-range the predicted values are almost the same as the numerical values.

The Markstein numbers are determined by taking the slope of the profiles displayed in figure 2 at $Ka = 0$. This is done for the numerical profile and for the theory of each type of flame. The results are presented in table 2. The difference between the values displayed in table 2 and the slopes in figure 2 is caused by the factor $Le_i$, which is used in the figure. However in the table the following definition is used:

$$\frac{m_{il}}{m_{il}^0} = 1 - \mathcal{M}Ka \,, \tag{26}$$

where $\mathcal{M}$ represents the Markstein number. As in figure 2, Markstein numbers evaluated using numerical results for $\Delta h$ and $\Delta Z_j$ are also presented. Table 2 confirms the results that were found in figure 2. The difference between the Markstein numbers found from the numerical simulations and the theoretical predictions are a good measure for the error. For ethane and propane the difference is smaller than 5%. However, the predictions for methane (typically 20%) are less accurate than the predictions for ethane and propane. To understand the reason for this, let us investigate the magnitude of the different contributions of the enthalpy, $c_h \Delta h$, and the different elements, $c_j \Delta Z_j$, to the value of the mass burning rate. This is displayed in figure 3. Note that the contributions of the enthalpy and chemical composition have the same sign in lean ethane/air and propane/air flames, while they have opposite signs in both methane/air flames. In the methane/air mixtures the different contributions partly cancel, which results in a relatively small overall preferential diffusion effect but a larger error. This also explains the higher accuracy in ethane and propane flames investigated in this study. The preferential diffusion effect for ethane as well as propane are larger than the preferential diffusion effect of the methane flames, as is commonly known. The same trend can also be seen in the individual Lewis-numbers of the fuels; the Lewis number of methane is closer to one than the Lewis numbers of ethane and propane. Concluding, as in most other studies, a neutral preferential diffusive behavior is observed

Table 2: Markstein numbers

| | methane | | ethane | propane |
|---|---|---|---|---|
| | $\phi = 0.8$ | $\phi = 0.9$ | $\phi = 0.8$ | $\phi = 0.8$ |
| Numerical simulation | 1.47 | 1.70 | 2.43 | 3.03 |
| Weak stretch theory | | | | |
| $\Delta h$ and $\Delta Z_j$ from numerical simulation | 1.39 | 1.52 | 2.55 | 3.38 |
| $\Delta h$ and $\Delta Z_j$ from Eqs. (24) and (25) | 1.27 | 1.41 | 2.34 | 3.01 |

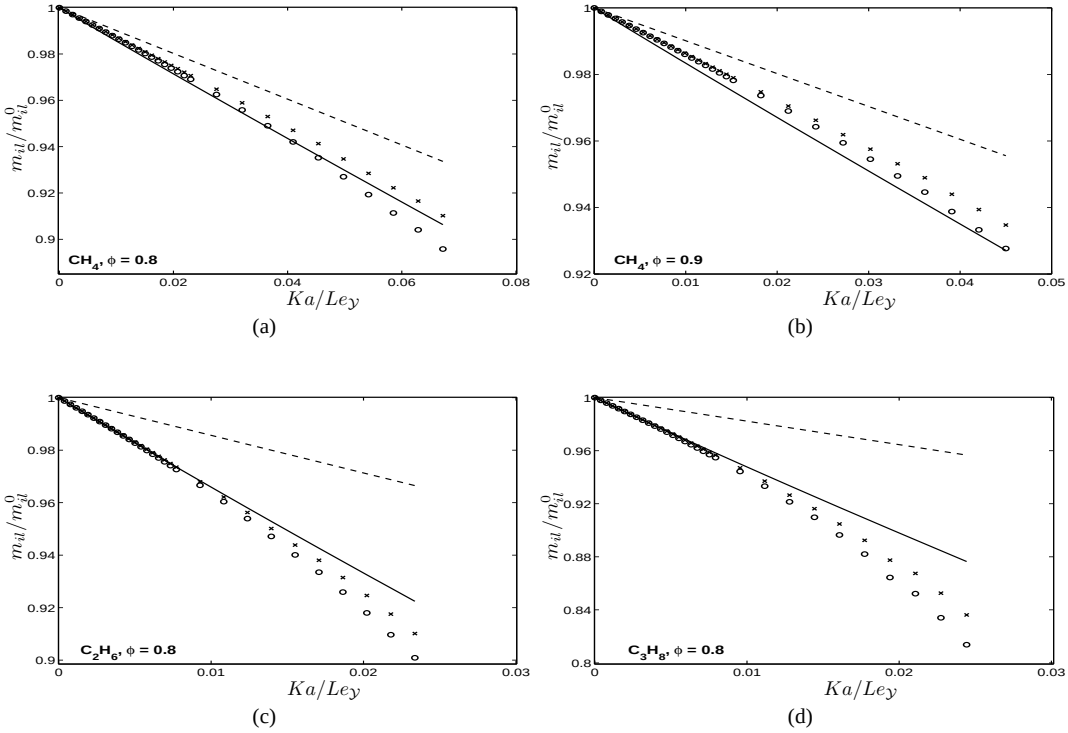


Figure 2: Prediction of $m_{il}$. Full line: numerical solution; dashed line: $Le_i = 1$. Weak stretch theory for $m_{il}$ using numerical results for $\Delta h$ and $\Delta Z_j$ ($\circ$) and weak stretch theory using $\Delta h_{il}$ and $\Delta Z_{j,il}$ from theory (Eqs. 22 and 23) ($\times$)

for lean methane/air flames and the influence of preferential diffusion increases with the fuel mass. A quantitative comparison of Markstein numbers with other values in the literature is not performed since different definitions are used by different authors. In addition it should be realized that the value of the Markstein number depends on the position in the flame, which makes a quantitative comparison even more difficult.

**Conclusions**

The model as introduced by De Goey and Ten Thije Boonkkamp [8], describes the mass burning rate of stretched flames with non-unit Lewis numbers. This model is adjusted to describe the mass burning rate at the inner layer position. The model proved to lead to an accurate description of the mass burning rate of stretched flames for the weak stretch limit. Several figures display the accuracy of this model. This new model includes more physics, like multi-species transport and the formation and destruction of radicals and intermediates. It is striking to see that the sensitivity coefficients of the different fuels and flames investigated in this study have the same order of magnitude. It requires more research to determine the physical background of this phenomenon. It is also shown that the inner layer is a better position to evaluate $\Delta h$ and $\Delta Z_j$ than the burnt side of the flame. Furthermore it can be seen that the mass burning rate of methane/air flames is more difficult to predict, because cancelation takes place. Different preferential diffusion contributions (expressed in enthalpy and elements or species and temperature) cancel each other out and the total preferential diffusion effect is relatively small. Under the assumptions of one-step chemistry, a single Lewis number and activation energy asymptotics well-known expressions can be found. ([14], [15]). Future work will focus on the effects of strong stretch in combination with preferential diffu-

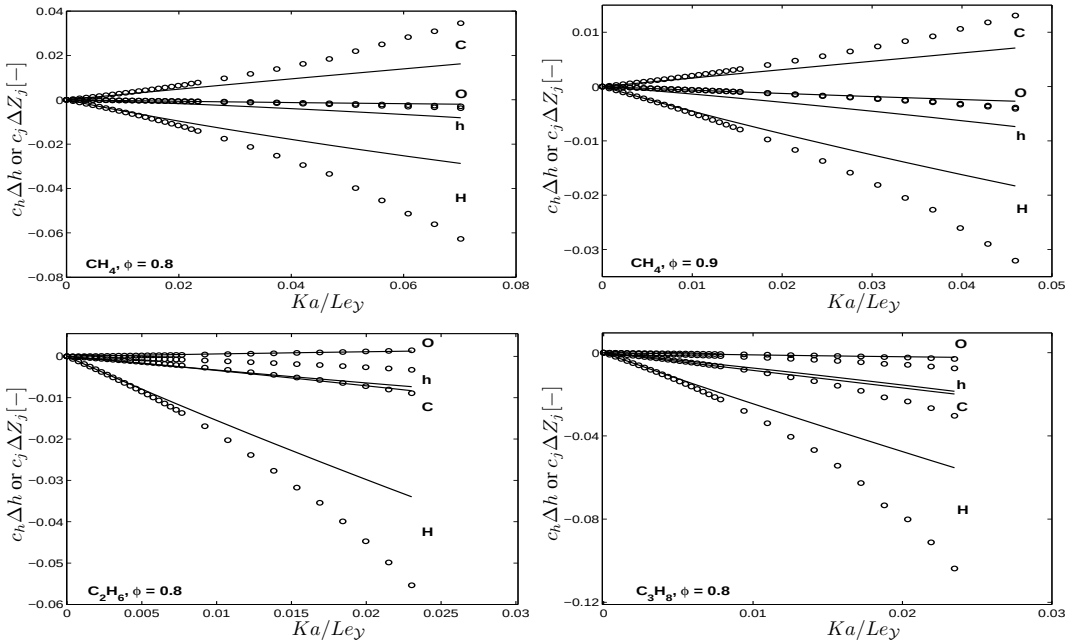


Figure 3: Contributions of preferential diffusion terms expressed in enthalpy and element mass fractions. Full line: numerical solution and weak stretch theory (○)

sion on the mass burning rate. This could make it possible to describe the mass burning rate of strongly stretched flames without solving the complete flame structure.

**References**


[1] B. Karlovitz, D.W. Denniston Jr., D.H. Knapschaefer, and F.E. Wells. *Fourth symposium on Combustion*, pages 613–620, 1953.

[2] G.H. Markstein. *Nonsteady Flame Propagation*. Pergamon Press, Oxford, 1964.

[3] J.D. Buckmaster. *Acta Astronautica*, 6:741–769, 1979.

[4] J.D. Buckmaster. *Q. J. Mech. Appl. Math.*, 35:249–263, 1982.

[5] M. Matalon. *Combust. Sci. Technol.*, 31:169–181, 1983.

[6] M. Matalon and B.J. Matkowski. *J. Fluid Mech.*, 124:239–259, 1982.

[7] S.H. Chung and C.K. Law. *Combust. Flame*, 72:325–336, 1988.

[8] L.P.H. de Goey and J.H.M. ten Thije Boonkkamp. *Combust. Flame*, 119:253–271, 1999.

[9] J.A. van Oijen and L.P.H. de Goey. *Combust. Theory and Modeling*, 6:463–478, 2002.

[10] J.A. van Oijen and L.P.H. de Goey. *Combust. Theory and Modeling*, 8:141–163, 2004.

[11] J.A. van Oijen, G.R.A. Groot, R.J.M. Bastiaans, and L.P.H. de Goey. A flamelet analysis of the burning velocity of premixed turbulent expanding flames. *Proc. Combust. Inst.*, 30(1):657–664, 2004.

[12] L.P.H. de Goey and J.H.M. ten Thije Boonkkamp. *Combust. Sci. Techn.*, 122:399–405, 1997.

[13] U. Maas and S.B. Pope. *Combust. Flame*, 88:239–264, 1992.

[14] G. Joulin and P. Clavin. *Combust. Flame*, 35:139, 1979.

[15] P. Clavin. *Prog. Energy Combust. Sci.*, 11:1–59, 1985.